Experimental investigation of saturation and convection of two-plasmon-decay instability in laser-produced plasmas

B. K. Sinha and S. R. Kumbhare
Laser Division, Bhabha Atomic Research Centre, Bombay 400 085, India

G. P. Gupta
Plasma Physics Division, Bhabha Atomic Research Centre, Bombay 400 085, India

(Received 5 April 1989)

Experiments were conducted on planar slab targets of carbon, aluminum, and copper using a 20-J 5-nsec, *s*- and *p*-polarized Nd:glass laser for the studies of saturation phenomena associated with two-plasmon-decay instability by monitoring the spectral profiles of $\frac{3}{2}\omega_0$ emissions at different laser intensities. It was observed that the emissions from carbon plasma showed the existence of wavelength-dependent saturation domain of the instability at and beyond a laser intensity of 10^{14} W/cm^2, but the emission from copper and aluminum did not show the saturation behavior. The existence or absence of saturation behavior is explained on the basis of excitation of various parametric decay instabilities modulated by damping processes in a plasma. The suitability of temperature diagnostics from the peak shifts of these emissions is also discussed.

I. INTRODUCTION

Although many theoretical as well as experimental workers have reported on the various aspects of two-plasmon-decay (TPD) instability in laser-produced plasmas, as monitored by $\frac{3}{2}\omega_0$ emissions, the influence of basic plasma processes on the observed spectral profiles of these emissions is not well understood.[1-12] Generally, the earlier authors have investigated the threshold of the instability,[12] the suitability of temperature diagnostics from $\frac{3}{2}\omega_0$ emissions,[3,7-10] and their spectral profiles,[5,10] but, still, the various conclusions are far from complete and they provide a great incentive for further theoretical investigation of the problem. It is well known that the pump-wave combination scattering by the parametrically excited Langmuir oscillations near the quarter-critical density ($n_c/4$) layer is responsible for the generation of $\frac{3}{2}\omega_0$ emissions, but it is not well known as to what the nature of the TPD instability is and whether the instability is convective or absolute and what its relative contribution to the generation of $\frac{3}{2}\omega_0$ emissions is and what role it plays as regards the saturation of these emissions as reported by the earlier workers.[12] Moreover, Aboites *et al.*[9] and Karttunen[11] have reported that the region of excitation of TPD instability and the region where the plasmons and light waves combine to produce the $\frac{3}{2}\omega_0$ emissions may not be the same. As a result, one has to consider the convection property of the plasmons, which gets modulated by the collisional and Landau damping processes.

In the present work we report the observations of saturated as well as unsaturated profiles of $\frac{3}{2}\omega_0$ emissions from plasmas produced from slab targets of carbon, aluminum, and copper using a 20-*J*, 5-nsec, *p*- as well as *s*-polarized Nd:glass laser. At a laser intensity of approximately 10^{14} W/cm^2, the emissions produced from the carbon target showed a saturated profile, whereas those produced from aluminum and copper did not. Moreover, it was noted that the emissions had a stronger tendency for saturation for the *p*-polarized light than for the *s*-polarized one. We have tried to explain the saturation phenomena on the basis of the onset of absolute TPD instability at a higher laser intensity. We have further considered the effect of Landau and collisional damping on the convection of the plasmons from the region of plasmon production to the region of generation of $\frac{3}{2}\omega_0$ emissions.

II. THEORETICAL CONSIDERATION

A. Type and nature of the instability

It is generally understood that there are mainly three processes that contribute to $\frac{3}{2}\omega_0$ emissions from laser-produced plasmas. Apart from TPD instability as mentioned in Sec. I, the second process that may contribute to the relevant emission is three-plasmon coupling, but this is generally regarded as a higher-order process.[13] Its probability was evaluated by Alexandrov,[14] who reported that three-plasmon-coupling contribution to $\frac{3}{2}\omega_0$ emission is negligibly small under the laser-produced plasma conditions. In the third process the parametric excitation of the plasmons may also be caused by stimulated Raman scattering (SRS). However, the TPD instability threshold is observed to be lower than that of SRS (Refs. 1, 15–17) if the density gradient scale length L near the $n_c/4$ layer is not very large, so that the following inequality holds true:

$$(k_{0v}L)^{1/6} < (c/V_e) , \tag{1}$$

where $k_{0v}=\omega_0/c$ is the pump wave number in a vacuum, c is the speed of light, $V_e=(k_B T_e/m_e)^{1/2}$ is the electron

thermal speed, k_B is the Boltzmann constant, and T_e and m_e are the electron temperature and mass. For typical experimental conditions, $k_{0v}L < (10^2 - 10^3)$, $T_e \sim 0.5$ keV and consequently the inequality as expressed in Eq. (1) is valid. To have a more quantitative picture one may estimate the ratio of laser intensity thresholds $(I_{\mathrm{TPD}})_{\mathrm{th}}$ and $(I_{\mathrm{SRS}})_{\mathrm{th}}$ for TPD and SRS instabilities, respectively, at the quarter-critical density layer from the expression given by Liu.[18] This can be written as

$$[(I_{\mathrm{TPD}})_{\mathrm{th}}/(I_{\mathrm{SRS}})_{\mathrm{th}}] = 3(k_{0v}L)^{1/3}(V_e/c)^2 \ . \tag{2}$$

Taking $L = 50$ μm and a typical value of T_e at the TPD threshold for carbon as 300 eV, this ratio can be estimated to be 1.176×10^{-2}, which leads to the fact that $(I_{\mathrm{SRS}})_{\mathrm{th}}$ is approximately 85 times larger than $(I_{\mathrm{TPD}})_{\mathrm{th}}$. Therefore, it is reasonable to assume that the SRS contribution to $\frac{3}{2}\omega_0$ emission, at the $n_c/4$ layer, is negligible in the range of laser intensities in which the experiments are being reported. Hence, the profiles of $\frac{3}{2}\omega_0$ emissions can be considered as due to the TPD instability.

It is further understood that in the case of TPD instability, which occurs near the quarter-critical density layer, the pump wave decays into two plasmons with frequencies $\approx \omega_0/2$, where ω_0 is the frequency of the incident laser. These plasmons undergo amplification in the unstable region in which the phase-matching conditions are approximately satisfied in an inhomogeneous plasma. The intensity of the amplified plasmons may either be saturated due to some nonlinear effects in the cases of both absolute and convective instabilities or limited due to a linear growth over a spatially limited region in the case of convective instability. The large-amplitude plasmons excited either by absolute or convective TPD instability may give rise to a variety of nonlinear effects,[19] thereby saturating their amplitudes. One of the important nonlinear processes observed in many experiments or invoked for the analysis of experimental results is the parametric decay of a plasmon into a plasmon of longer wavelength and a phonon.[20–23]

Now, it is important to consider the nature of the instability. Liu and Rosenbluth[18] have noted that the TPD instability in an inhomogeneous plasma is absolute. Rosenbluth[15] has shown that the TPD instability in an inhomogeneous plasma may be absolute or convective provided the wave number mismatch $\Delta k = [k_0(x) - k_1(x) - k_2(x)]$ in the unstable region is linear or quadratic in x, where x is the direction of inhomogeneity and k_0, k_1, and k_2 are the wave numbers of the pump wave and the excited plasmons. Although for a given laser-produced plasma it is difficult to find out whether Δk is linear in x or not, Rosenbluth[15] states that it does not appear possible to rule out the linear nature of Δk in the TPD process and hence, the TPD instability is likely to be convective. Following Rosenbluth, Bychenkov *et al.*[1] have considered the TPD instability convective in nature.

When we consider the amplitude saturation of plasmons, one may note that the plasmons should grow to their nonlinear limit. Typically, five e folds are required for nonlinear saturation.[24,25] Let us estimate the characteristic time or length for five e folds in a typical plasma. The TPD growth rate in an inhomogeneous plasma is given as[18,26]

$$\gamma = \frac{k_0 v_0}{2} - \frac{3\sqrt{3} k_0 k_y V_e^2}{8\omega_p} - \frac{\omega_p}{4k_y L} \tag{3}$$

where $v_0 = eE_0/m\omega_0$ is the electron quiver velocity, ω_p is the electron plasma frequency, and k_y is the wave number of either plasmon in the direction of the electric field of the incident laser. In practical units, the value of v_0 is expressed as[27] $v_0/c = 4.27 \times 10^{-10} \lambda_{\mu m} I_0^{1/2}$, where $\lambda_{\mu m}$ is the vacuum laser wavelength in μm and I_0 is the laser intensity in W/cm^2. Simon *et al.*[27] have discussed, in detail, the threshold, wavenumber, and frequency of the TPD instability in an inhomogeneous plasma for a normally incident pump wave. There is a critical value of k_y for the onset of the instability[27] depending on the value of $\beta = 1.41 \times 10^{14} T_{\mathrm{keV}}^2 / I_0 \lambda_{\mu m}^2$ where T_{keV} is the electron temperature in keV. Above the threshold, the growth rate is found to vary smoothly with k_y, peaking at some intermediate value. The frequency shift from the exact $\omega_0/2$ value of the unstable spectrum of plasmons also varies with k_y. For our laser of 1.0641 μm wavelength and $I_0 = 1.5 \times 10^{14}$ W/cm^2, with an estimated electron temperature of 600 ± 60 eV for carbon, the value of β turns out to be ≈ 0.3. Using the threshold k_y expression under the small-β approximation given by[27] $(k_y/k_0)^2 = 1/6\beta$ and noting that $k_0 = 3^{1/2}\omega_p/c$ at the $n_c/4$ layer, we obtain $k_y \lambda_D \approx 0.04$ at the onset of the instability for the laser intensity of 1.5×10^{14} W/cm^2. Here λ_D is the Debye length. The minimum growth rate in the unstable k_y spectrum is estimated using $k_y \lambda_D = 0.04$ and the other values at the $n_c/4$ layer in Eq. (3), which gives $\gamma_{\mathrm{min}} = 1.6 \times 10^{12}$ sec^{-1}. Consequently, the five e-fold growing time $(= 5/\gamma)$ is approximately 3×10^{-12} sec. Other plasmons in the unstable spectrum will take comparatively less time to grow five e fold. As the time taken by the TPD plasmons in the unstable spectrum is much smaller than the laser pulse duration, the plasmons excited by the absolute TPD instability grow until saturation by the parametric decay of plasmons into secondary plasmons and phonons, the process which provides an efficient saturation mechanism for TPD plasmons.[21] In the case of convective TPD instability, whether the plasmons grow to their nonlinear limit or not is assessed from the characteristic five e-fold growing length L_{ch}, which is estimated from $L_{\mathrm{ch}} = (5/\gamma) V_g$, where V_g is the group velocity of the plasmons and is expressed in the limit $k\lambda_D \ll 1$ as

$$V_g = 3V_e(k\lambda_D)/[1 + \tfrac{3}{2}k^2\lambda_D^2] \ , \tag{4}$$

where k is the plasmon wave number. For $I_0 = 1.5 \times 10^{14}$ W/cm^2, with an estimated plasma temperature of 600 ± 60 eV for carbon, typical excited plasmon wave numbers fall in the range[11] of $0.05 < k\lambda_D < 0.2$. This gives a characteristic length of $L_{\mathrm{ch}} \approx 5 - 18$ μm. From the present analysis it follows that the plasmon saturation can take place even for convective TPD instability provided the unstable region is greater than $5 - 18$ μm. But,

the unstable region whose spatial extent[15] in an inhomogeneous plasma is of the order of $(\Delta k/\Delta x)^{-1/2}$ is about less than 1 μm in our laser-target experiments and hence, is insufficient for plasmon saturation. We thus conclude that the plasmons do not saturate in the case of convective TPD instability under the conditions of our interest. However, to decide the nature of the instability, it is necessary to estimate the intensity thresholds for convective and absolute TPD instabilities. Rosenbluth[15] has given the threshold for the convective TPD instability as

$$(2/3)\pi^2(e/mc^2)^2(mc^2/T_e)I_0L/\omega_0>1 \ . \tag{5a}$$

Putting the constants in the above equation, the threshold condition can be written in practical units as

$$I_{\rm cth}\ ({\rm W/cm^2})>1.6\times10^{15}(T_{\rm keV}/\lambda_{\mu m}L_{\mu m}) \ . \tag{5b}$$

The threshold condition for absolute TPD instability is given by Boyd[28] as

$$I_{\rm ath}\ ({\rm W/cm^2})>2.0\times10^{16}(T_{\rm keV}/\lambda_{\mu m}L_{\mu m}) \ , \tag{6}$$

which is an order of magnitude higher than that for the convective instability. For $L=50$ μm, $\lambda_{\mu m}=1.0641$ μm, and T_e (keV)$=0.3$, the convective and absolute thresholds come out to be 8.4×10^{12} and 1.1×10^{14} W/cm^2, respectively. These are the considerations which will be useful when we consider the profiles and saturation phenomena associated with the $\frac{3}{2}\omega_0$ emissions.

B. The Landau and collisional damping

It is generally understood that in the convective TPD instability, the electron plasma waves with frequency $\approx\omega_p\approx\omega_0/2$ get amplified spatially during the propagation through the unstable region and come out with an amplified intensity.[1,11,15] These amplified plasma waves convect to the region where the combination scattering conservation laws are satisfied and $\frac{3}{2}\omega_0$ harmonic is emitted.[11] Between the unstable region of TPD instability and the harmonic generation region, the electron plasma waves are damped due to collisional or Landau damping or both, depending upon their wave numbers. Thus spatial damping of electron plasma waves plays an important role in the emitted harmonic spectrum.

The temporal, collisional damping rate $(\Gamma_p)_C$ of the electron plasma wave is expressed[29] as $(\Gamma_p)_C=\nu_{ei}/2$, where ν_{ei} (in sec^{-1}) is the electron-ion collision frequency and can be evaluated from the equation[30]

$$\nu_{ei}=5.2\times10^{-6}\bar{Z}n_eT_e^{-3/2}\ln\Lambda \ , \tag{7}$$

where

$$\Lambda=1.24\times10^7T_e^{3/2}/(\bar{Z}^{3/2}n_e^{1/2}) \ . \tag{8}$$

Here $\bar{Z}$ represents the average charge state of the ion, T_e the electron temperature in K, n_e the electron density in m^{-3}, and $\ln\Lambda$ the Coulomb logarithm. The temporal Landau damping rate $(\Gamma_p)_L$ of the electron plasma waves is given as[29]

$$(\Gamma_p)_L=(\pi/8)^{1/2}e^{-3/2}(\omega_p/k^3\lambda_D^3)e^{-1/(2k^2\lambda_D^2)} \ . \tag{9}$$

This relation is valid for $k\lambda_D\ll1$, i.e., for wavelengths much larger than the Debye length. If the wavelength approaches λ_D, the damping rate of the plasma waves is of the same order of magnitude as the frequency of the waves. Consequently, plasma waves with the wavelength equal to or less than the Debye length are nonexistent in the plasma. As the plasma wave propagates in the plasma and takes a finite time, it decays in space. The spatial damping rate K_p of the plasma wave can be estimated from the temporal damping rate from the relation

$$K_p=\Gamma_p/V_g \ . \tag{10}$$

Using the expression for collisional and Landau damping as given above, calculations of temporal and spatial damping rates have been made at temperature 0.5, 1.0, and 1.5 keV by taking $n_c/4=2.5\times10^{26}$ m^{-3}. The average ionization state $\bar{Z}$ has been obtained from the empirical relation deduced by Shearer and Barnes[31] and checked with the works reported by Mosher.[32] Figure 1 shows the variation of the temporal damping rate Γ_p of the plasma waves normalized with respect to ω_p due to collisional and Landau effects, as a function of the normalized wave number (kc/ω_p), for carbon and copper plasmas at different values of T_e. It is seen from the figure that the temporal collisional damping is independent of the wave number, whereas Landau damping is negligible below a certain wave number which corresponds to $k\lambda_D\approx0.2$ and increases significantly thereafter, with an increase in k. Thus collisional damping is dominant for plasma waves with wave numbers satisfying the inequality $k\lambda_D<0.2$. The collisional damping is smaller for higher electron temperatures at a particular value of $\bar{Z}$ and is larger for higher values of $\bar{Z}$ at a particular temperature. On the contrary, Landau damping is larger for higher T_e and is independent of $\bar{Z}$.

Figure 2 shows the variation of normalized spatial damping rate (K_pc/ω_p) of the electron plasma waves due to Landau and collisional effects, as a function of the normalized wave number (kc/ω_p), for carbon and copper plasmas at different values of T_e. It is evident from the figure that unlike the temporal collisional damping, the spatial collisional damping becomes dependent on the wave number, decreasing with increasing wave number. Except for this variation, the nature of the spatial damping remains the same as that of temporal damping. With a view to applying these damping calculations to explain the observed behavior of the scattered $\frac{3}{2}\omega_0$ harmonic peak intensity as a function of laser intensity, it will be useful to consider the spatial damping rates of the plasma waves in carbon, aluminum, and copper plasmas at a laser intensity of 10^{14} W/cm^2 where the intensity saturation for carbon only is observed. Corresponding to this laser intensity electron temperatures for carbon, aluminum, and copper were estimated to be 500±50, 1100±100, and 1200±100 eV, respectively, as explained in Sec. III. The corresponding values of $\bar{Z}$ are estimated to be nearly 6, 12, and 20 for C, Al, and Cu, respectively. As the wave number of the plasma waves excited by the convective TPD instability is somewhat longer than that of the incident laser, the normalized wavenumber

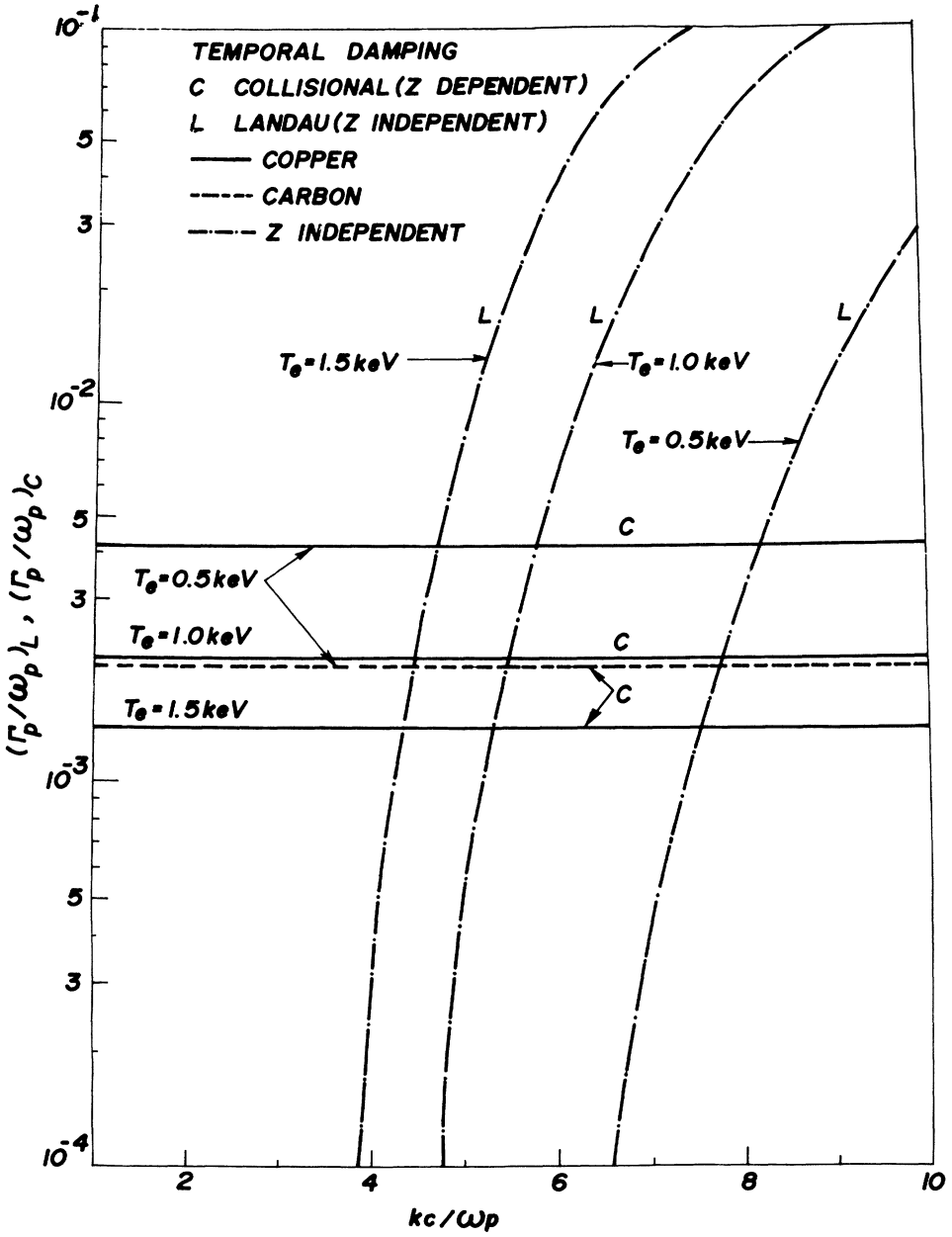

FIG. 1. Normalized temporal damping rate (Γ_p/ω_p) of electron plasma waves due to Landau and collisional effects as a function of the normalized wave number (kc/ω_p) in carbon and copper plasmas at different values of the electron temperature T_e.

(kc/ω_p) of the plasma waves lies beyond 2. Because the observed harmonic intensity variation is found to show Z dependence (see Sec. III), it is the collisional damping which is dominant and thus the normalized wave number lies somewhat around 2. From Fig. 2 it is evident that the spatial damping rate in carbon plasma ($T_e = 500$ eV) is about three times more than that in copper plasma ($T_e = 1.2$ keV) at $kc/\omega_p = 2$. It is also found that at the same intensity the damping rate in aluminum plasma (not shown in Figs. 1 and 2) is slightly lower than but close to that in copper plasma. The e-folding damping length in carbon plasma is found to be approximately 1 μm, whereas it is about 3 μm in copper plasma and about 3.5 μm in aluminum plasma. Thus the plasma waves in carbon plasma are much more damped than those in copper and aluminum plasmas.

III. THE EXPERIMENT

The experiments were conducted using a 20-J 5-nsec, 1.0641-μm Nd:glass laser system which had a neodymium-doped yttrium aluminum garnet (Nd:YAG) oscillator. The schematic diagram of the experimental setup is shown in Fig. 3(a). The incident beam was both s

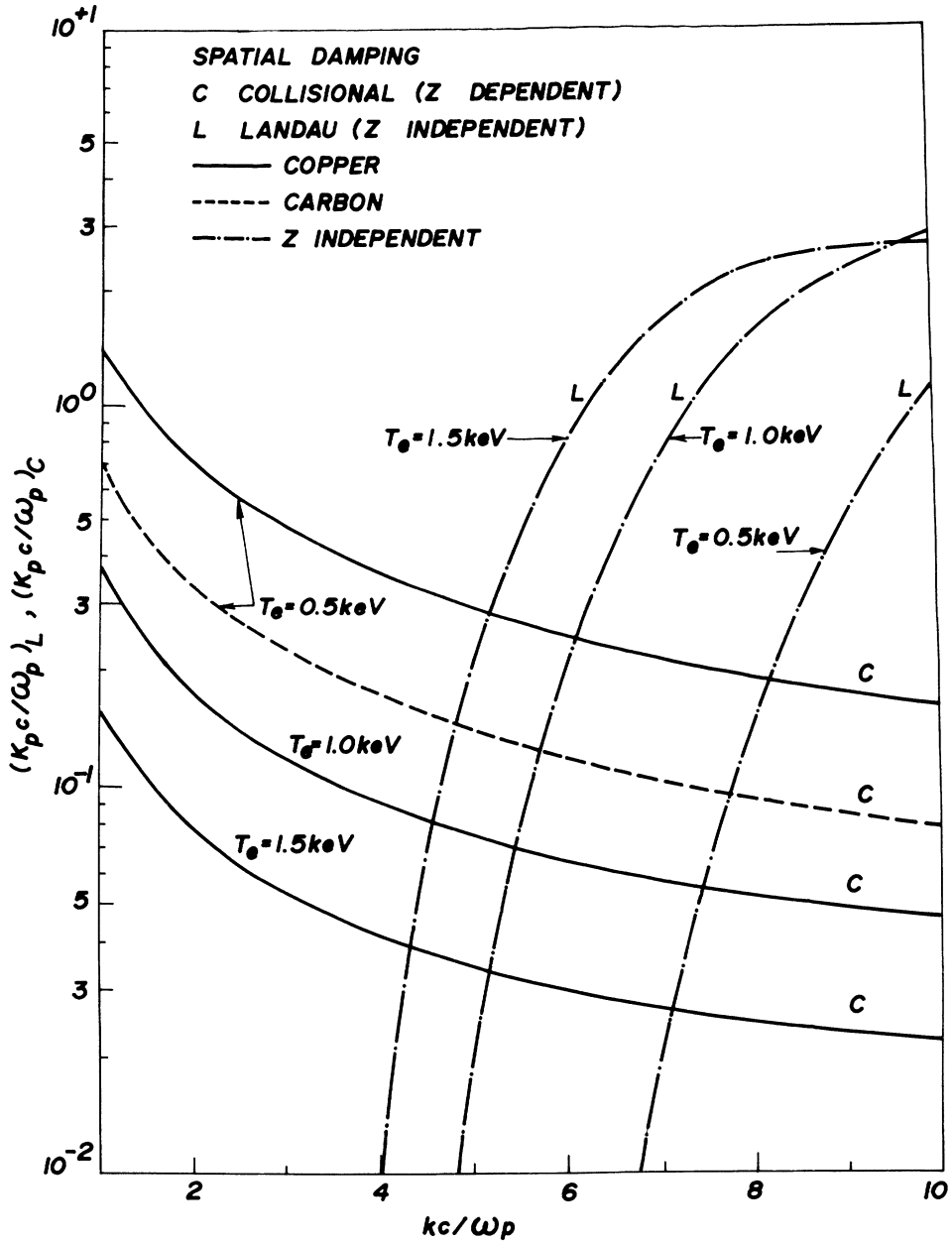

FIG. 2. Normalized spatial damping rate ($K_p c/\omega_p$) of electron plasma waves due to Landau and collisional effects as a function of normalized wavenumber (kc/ω_p) in carbon and copper plasmas at different values of the electron temperature T_e.

and p polarized. Here s and p polarization have been taken to mean laser polarization with respect to the plane of incidence, that is, the plane containing the target normal and the laser wave vector. The pump beam was incident on vertically positioned slab targets of the carbon, aluminum, and copper such that the laser beam through the center of the lens was normally incident and the beam through the outermost radius of the lens had an incident angle of approximately $\pi/10$, giving an average angle of incidence $\pi/20$. The horizontal plane gave the plane of incidence and the plane of p polarization. The scattered light was observed, in the plane of incidence, at an angle of $3\pi/4$ to the positive direction of the beam passing through the center of the lens. The state of laser polarization, the density gradient vector and the propagation vectors of incident and scattered beam are shown in Fig. 3(b). The plane of polarization of the laser beam was made either p or s, using a half-wave plate. The detector system consisted of a Pacific Instruments Inc. MP 1018B grating monochromator, coupled with an RCA-7265 photomultiplier tube with an S-20 response, and a Tektronix 7834 storage oscilloscope. The scattered radiation

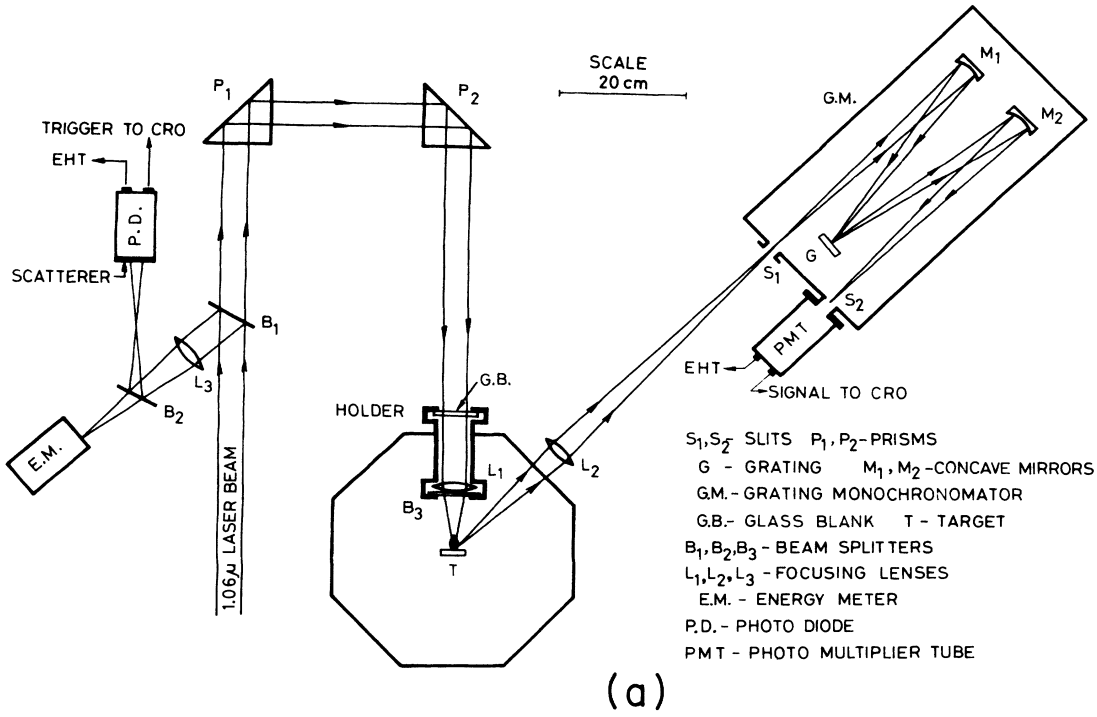

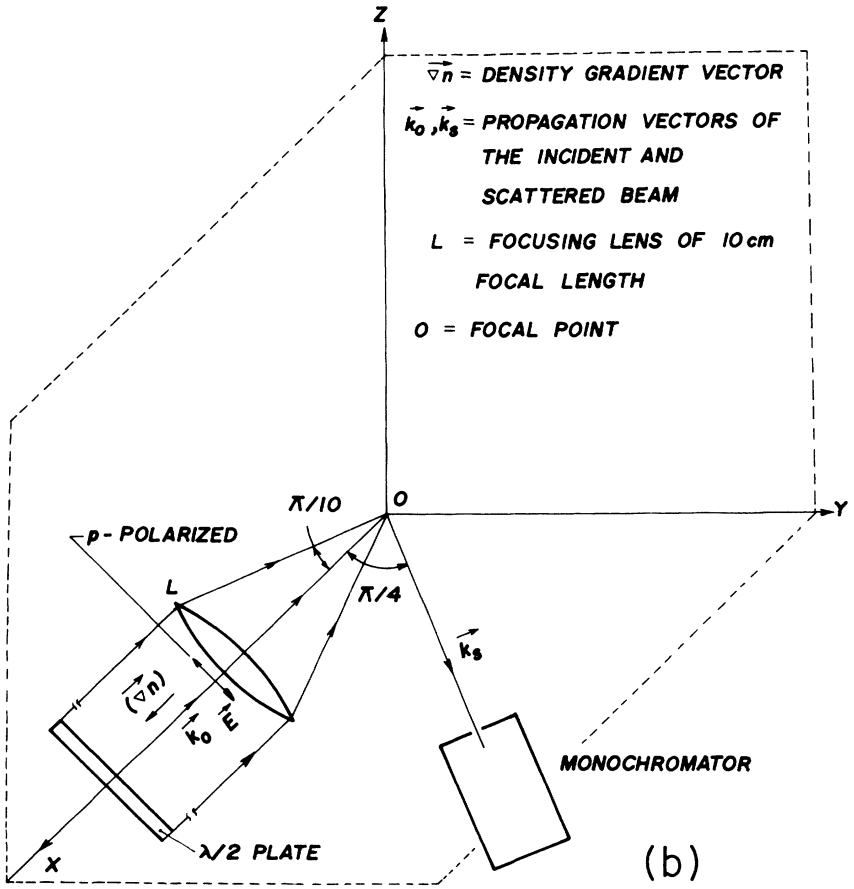

FIG. 3. (a) Schematic diagram of the experimental setup. (b) Schematic diagram showing the position of the focusing lens and the vectors representing polarization, density gradient, and incident and scattered beam propagation.

was measured with an accuracy of ± 0.5 Å and was collected approximately from the $n_c/4$ layer. An aspheric $f/1.33$ lens was used to focus the beam onto the target. Laser intensity was varied by varying the input pump energy density of the different amplifier stages keeping the focal spot diameter constant. Intensity measurements in the focal plane gave a focal spot diameter R of (40 ± 5) μm. Density scale length in the underdense region was estimated to be (45 ± 5) μm which is nearly the same as the focal spot diameter. The scale length was estimated using a 10 μm-resolution pinhole camera and the usual Abel inversion technique and was checked using interferometric technique. This estimation is in agreement with the expansion model discussed by Mora,[33] where he states that for laser-plasma experiments such that $C_s\tau > R$, the plasma expansion is spherical, instead of planar, where C_s and τ are ion-acoustic speed and laser pulse duration, respectively. In that case, L is expected to be of the order of R, irrespective of the target material. Our calculations show that the values of $C_s\tau$ are 600, 765, and 740 μm for carbon, aluminum, and copper, respectively, which satisfy the above criterion. Electron temperatures were estimated using the two-foil ratio technique.[34,35] It is to be noted that, at a laser intensity of approximately 10^{14} W/cm^2, aluminum and copper gave higher temperatures of (1.1 ± 0.1) and (1.2 ± 0.1) keV, respectively, than that of carbon which was estimated to be (0.5 ± 0.5) keV. Hydrodynamic simulations of Turner *et al.*[3] indicate that the underdense plasma temperature is higher for high-Z targets due mainly to their lower thermal conductivity and lower hydrodynamic losses. Moreover, Tabatabaei and MacGowan[36] reported a temperature of 1 keV for aluminum plasma at 1.0×10^{14} W/cm^2 from theoretical as well as experimental estimates, which is in agreement with our observations.

IV. EXPERIMENTAL RESULTS

The experimental results on the spectral profiles of $\frac{3}{2}\omega_0$ emissions and their intensity variation as a function of laser intensity can be primarily classified into results from low- and high-Z targets. The results from low-Z targets are those obtained from carbon and they are displayed in Figs. 4–7. The results from high-Z targets are those obtained from copper and aluminum and they are shown in Figs. 8–11 and in Figs. 12 and 13, respectively. The polarization states of the pump beam are also shown in the figures themselves. In the present experiments only the red satellite in the harmonic spectrum was obtained. It is understood that the spectrum of the backscattered $\frac{3}{2}\omega_0$ emission, in general, consists of a doublet in laser-plasma interaction experiments on solid targets and, as a result, the blue as well as red satellites in the backscattered $\frac{3}{2}\omega_0$ emission may be generated.[11] This is due to the reflection of either the forward propagating $\frac{3}{2}\omega_0$ radiation from its own critical density $n_c' = 9n_c/4$ or the forward propagating $\omega_0/2$ plasmon from the interior of the plasma. It may also further be generated if the reflected laser light from the n_c layer is intense enough to excite the TPD instability. In our experimental situation, the primary possible cause that may give rise to a blue satellite is the presence of the $9n_c/4$ layer. In such a situation, the intensity of the forward propagating $\frac{3}{2}\omega_0$ photon, which is typically smaller than 1% of the incident laser intensity,[37] falls in the linear regime and gets significantly reduced due to the inverse bremsstrahlung absorption during the passage of $\frac{3}{2}\omega_0$ photon up to the $9n_c/4$ layer and back. Hence, one may not record the blue peak, as in our case, or may record a faint blue peak as observed in some experiments,[38] depending on whether the spectroscopic resolution is inadequate or adequate, respectively.

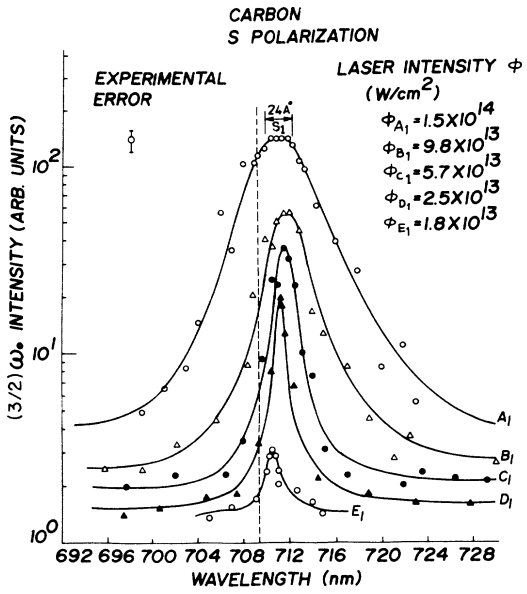

FIG. 4. Spectral profile of $\frac{3}{2}\omega_0$ emissions at different laser intensities for a carbon plasma when the pump beam is s- polarized.

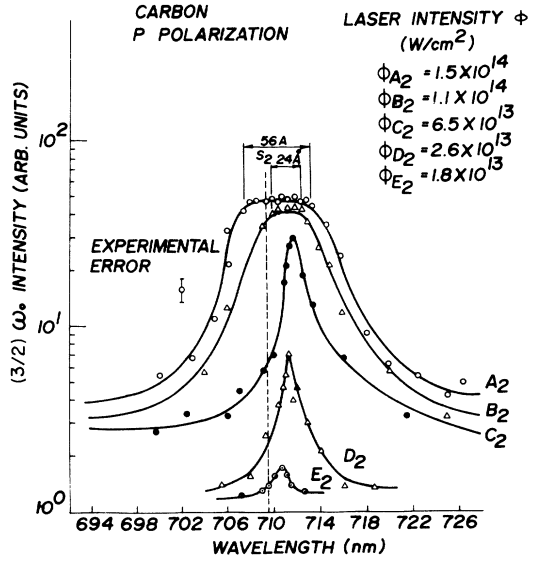

FIG. 5. Spectral profile of $\frac{3}{2}\omega_0$ emissions at different laser intensities for carbon plasma when the pump beam is p polarized.

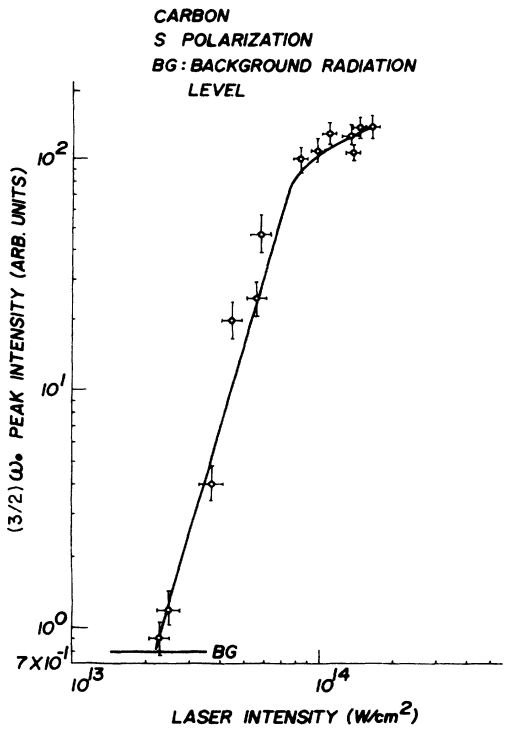

FIG. 6. Variation of the peak intensity of $\frac{3}{2}\omega_0$ emissions from carbon plasma as a function of laser intensity. The pump beam is s polarized.

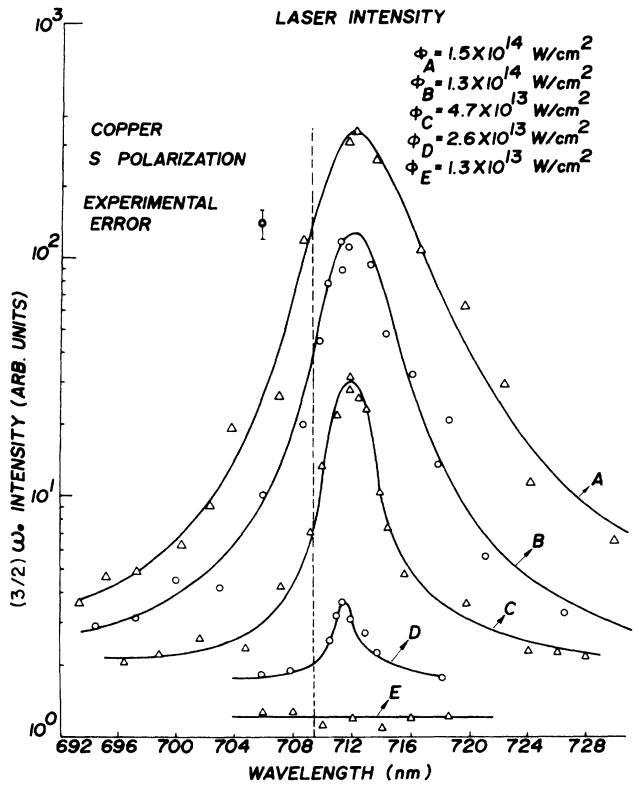

FIG. 8. Spectral profile of $\frac{3}{2}\omega_0$ emissions at different laser intensities ϕ for copper plasma. The pump beam is s polarized.

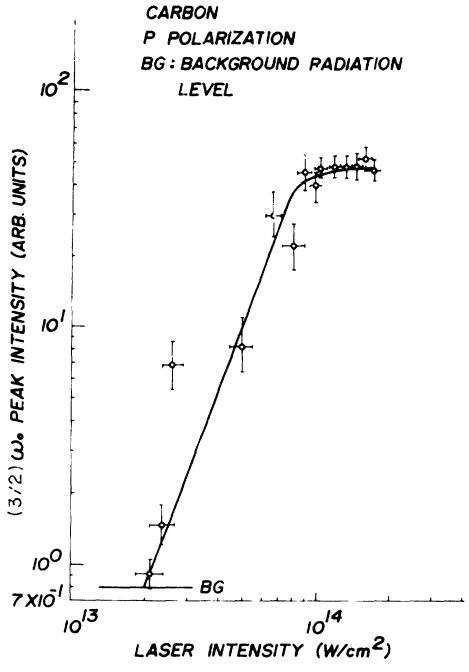

FIG. 7. Variation of the peak intensity of $\frac{3}{2}\omega_0$ emissions from carbon plasma as a function of laser intensity. The pump beam is p polarized.

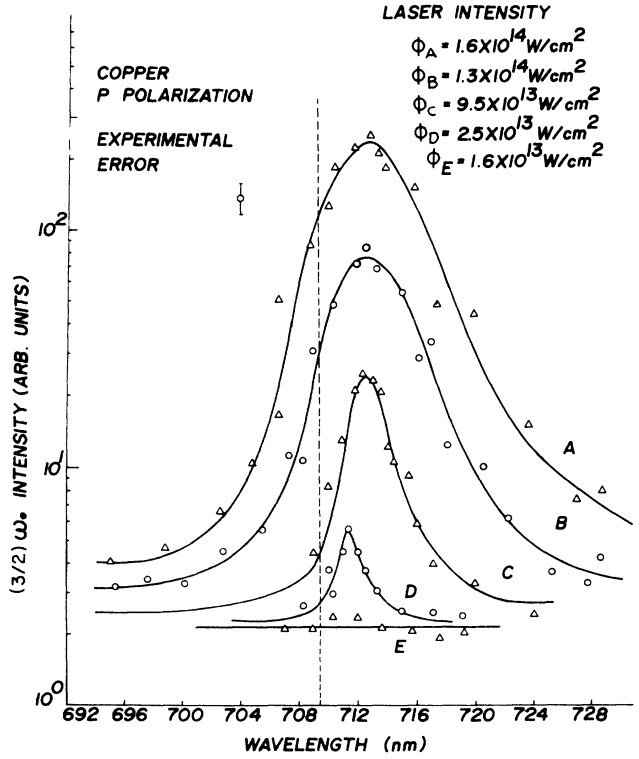

FIG. 9. Spectral profile of $\frac{3}{2}\omega_0$ emissions at different laser intensities ϕ for copper plasma. The pump beam is p polarized.

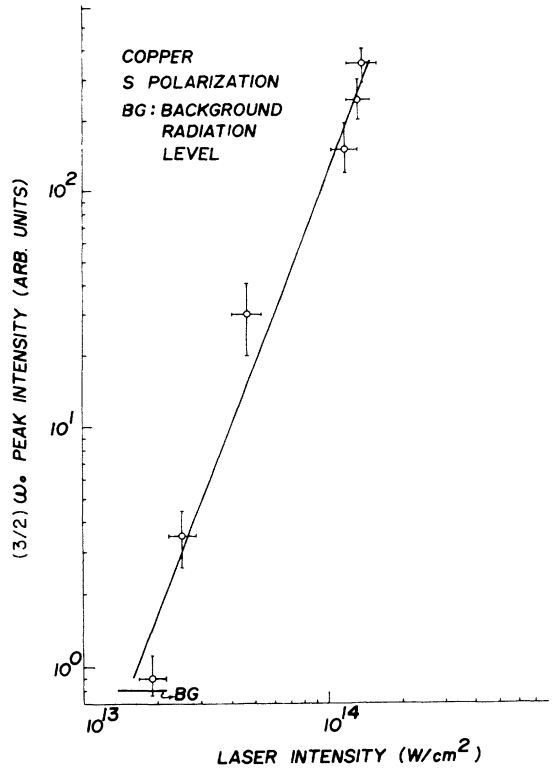

FIG. 10 Variation of $\frac{3}{2}\omega_0$ peak intensity for copper plasma as a function of laser intensity. The pump beam is s polarized.

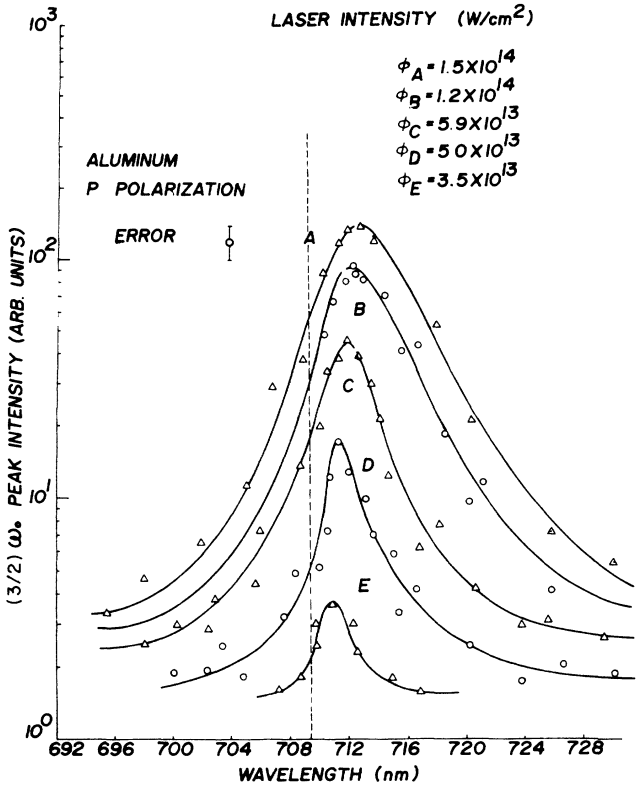

FIG. 12. Spectral profile of $\frac{3}{2}\omega_0$ emissions at different laser intensities for aluminum plasma. The pump beam is p polarized.

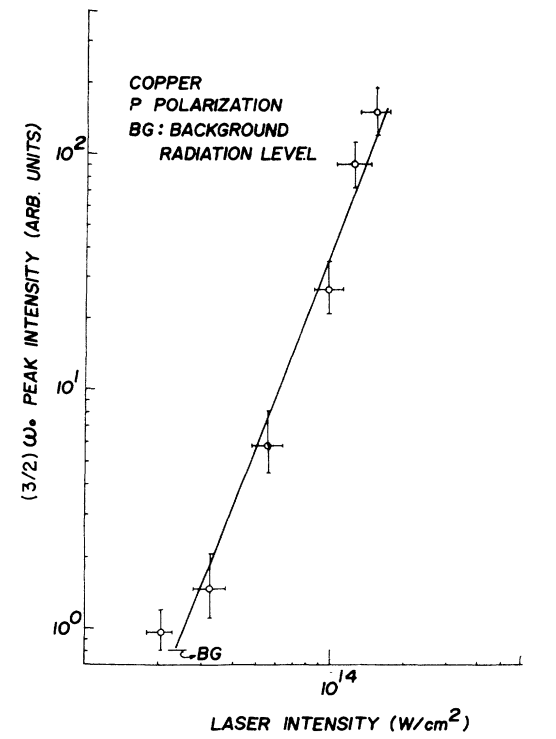

FIG. 11. Variation of $\frac{3}{2}\omega_0$ peak intensity for copper plasma as a function of laser intensity. The pump beam is p polarized.

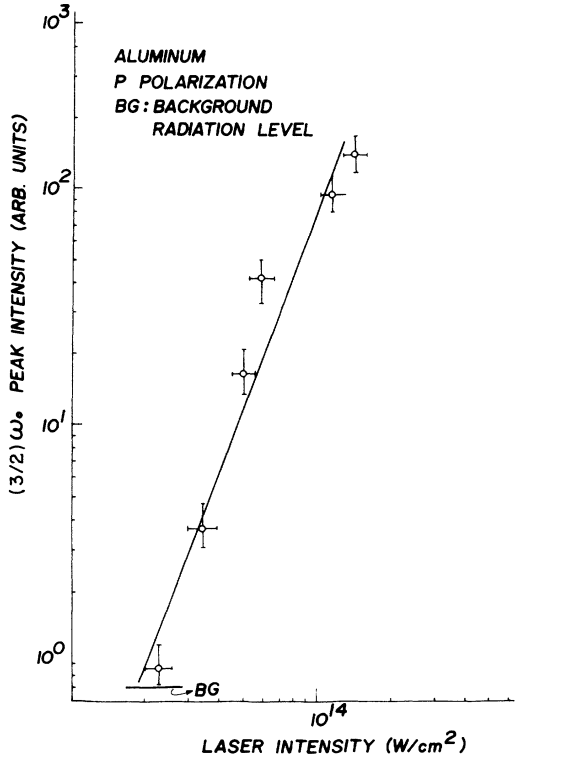

FIG. 13. Variation of $\frac{3}{2}\omega_0$ peak intensity for aluminum plasma as a function of laser intensity. The pump beam is p polarized.

In Figs. 14 and 15 the observed shifts of the red-satellite peaks from the exact $\frac{3}{2}\omega_0$ harmonic (7094 Å) are shown as a function of laser intensity for carbon and copper plasmas, respectively. These observed peak shifts are useful to discuss the theoretical prediction of Bychenkov *et al.*[1] as there seems to be no unanimous opinion as regards the suitability of these peak shifts for temperature diagnostics.[8,39,40]

Figures 4 and 5 show the profiles of $\frac{3}{2}\omega_0$ emissions for *s*- and *p*-polarized light, respectively, for carbon plasma. The curves B_1, C_1, D_1, and E_1 (Fig. 4) show the unsaturated profiles at laser intensities of 9.8, 5.7, 2.5, and 1.8×10^{13} W/cm^2, respectively. The curve A_1, at a laser intensity of 1.5×10^{14} W/cm^2, shows a wavelength-dependent saturated profile. The typical error bars are also shown in the figures. The profile (curve A_1) is flat over a region S_1 of 24 Å around the peak. It is also to be noted that the wavelengths corresponding to the peaks of emissions shift toward the lower-wavelength side at lower laser intensities, as expected. Similar results are plotted in Fig. 5 where the two curves A_2 and B_2 show wavelength-dependent saturation at laser intensities of 1.5 and 1.1×10^{14} W/cm^2, respectively. The curves C_2, D_2, and E_2 are in the nonsaturation regime of laser intensity. It can be noted that the profiles A_2 and B_2 have wavelength saturation domains S_2 and S_3 of 56 and 24 Å, respectively, that is to say, the saturation effects are much more pronounced in the case of *p*-polarized light than that in the case of *s*-polarized light at approximately the same laser intensity. They are furthermore pronounced at a higher intensity as shown by curves A_2 and B_2 of Fig. 5, which is expected.

Figures 6 and 7 show the variation of the peak intensities of $\frac{3}{2}\omega_0$ emissions as a function of laser intensity for *s*- and *p*-polarized light. The results obtained in Fig. 7 are very similar to the results reported earlier for *p*-polarized light.[12] The results obtained in Figs. 4–6 have not been reported so far. When we compare both Figs. 6 and 7 we note that the intensity saturation of $\frac{3}{2}\omega_0$ emissions, and hence the two-plasmon-decay instability, even for *s*-polarized light, does take place, but it is less pronounced than that due to *p*-polarized light.

Similar results as in Figs. 4 and 5 are displayed in Figs. 8 and 9 for copper but here one notes that there is no evidence of saturation of $\frac{3}{2}\omega_0$ emissions even at a laser intensity of 1.5×10^{14} W/cm^2 and even for *p*-polarized light (Fig. 9). We have further displayed the variation of the peak intensity of $\frac{3}{2}\omega_0$ emissions as a function of laser intensity in Figs. 10 and 11 for copper also. These figures (Figs. 10 and 11) demonstrate the complete absence of saturation phenomena for copper as we have seen in Figs. 4–7 for carbon. To confirm the results obtained on copper, an aluminum target was used and the results are displayed in Figs. 12 and 13 for *p*-polarized light only, as we have seen that *p* polarization has a stronger tendency to cause saturation effects. The results of Figs. 8–13 show that under the reported experimental conditions, $\frac{3}{2}\omega_0$ emissions from high-Z targets do not show saturation behavior in contrast to the results obtained from low-Z carbon targets and reported in Figs. 4–7.

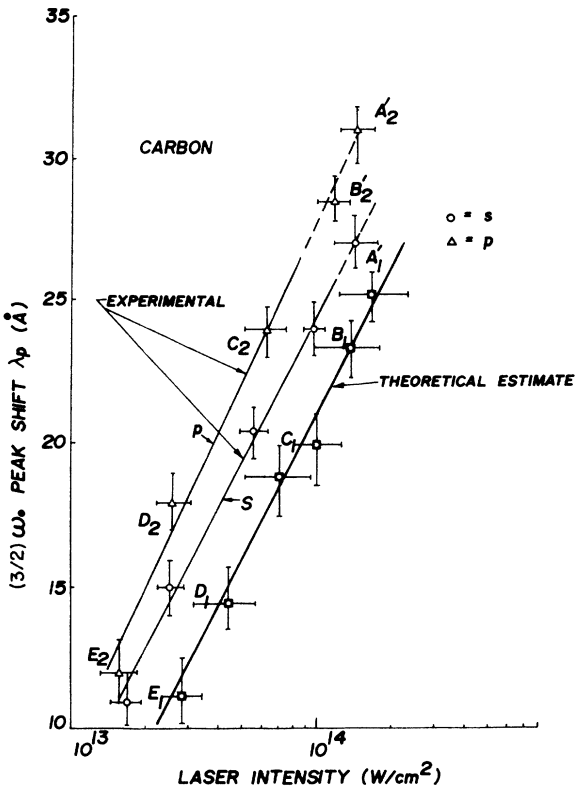

FIG. 14. Experimental and theoretical peak shifts of $\frac{3}{2}\omega_0$ emissions as a function of laser intensity for carbon.

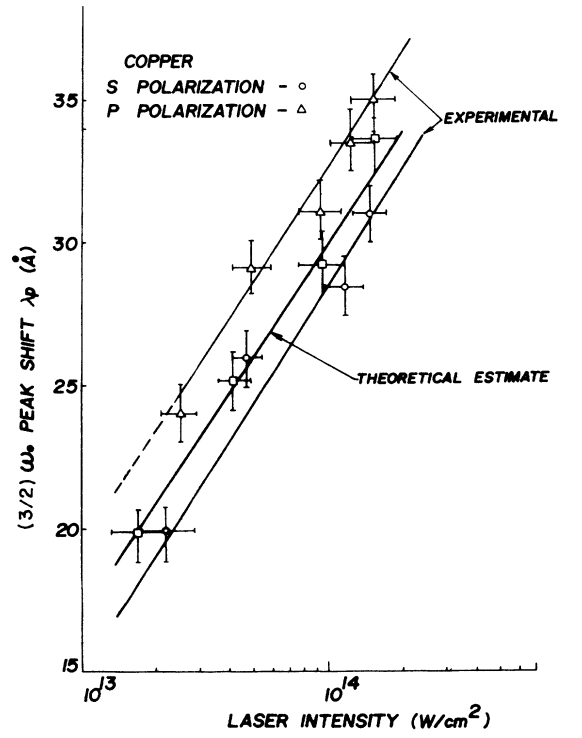

FIG. 15. Experimental and theoretical peak shifts of $\frac{3}{2}\omega_0$ emissions as a function of laser intensity for copper.

In Figs. 14 and 15 the observed and theoretically estimated peak shifts of $\frac{3}{2}\omega_0$ emissions from the exact $\frac{3}{2}\omega_0$ harmonic, as a function of laser intensity, are shown for carbon and copper, respectively. In the case of carbon when the saturation sets in, the profile becomes flat at and around the peak. In such cases we have taken the longer-wavelength end of the flat profile and plotted the values A_1', A_2' and B_2' as shown in Fig. 14. The discussion follows in the subsequent section. The results from the aluminum target were also obtained, and generally they support the conclusions obtained from copper. The error bars in the theoretical estimate arise because we have taken the experimental estimate of T_e at the given laser intensities for estimating the theoretical peak shift from the formulation given in Sec. V.

V. DISCUSSION

The experimental results reported in Sec. IV provide three very significant results in the field of laser-plasma interaction. The first is the observation of the existence of a wavelength-dependent saturation domain in low-Z targets represented by carbon with a preferentially higher tendency of saturation for a p-polarized laser pump beam. The second result represents the absence of saturation behavior of $\frac{3}{2}\omega_0$ emissions from high-Z targets like copper and aluminum in the same regime of laser intensity as that observed for carbon. The third result is reasonably good agreement of the observed peak shifts with those predicted by the detailed convective TPD instability theory of Bychenkov *et al.*[1]

Now, let us consider the saturation phenomena associated with the emissions from carbon. So far no workers have been able to explain the saturation phenomena taking into account the various processes involved in the formation of $\frac{3}{2}\omega_0$ emissions. As discussed in the theoretical consideration of Sec. II, we have noted that for the present experimental conditions the thresholds for convective and absolute TPD instabilities are 1.4×10^{13} and 1.1×10^{14} W/cm^2, respectively. Therefore, curves B_1, C_1, D_1, and E_1 of Fig. 4 and curves C_2, D_2, and E_2 of Fig. 5 may be taken to be due to convective TPD instability from the considerations of the threshold condition. Moreover, as per the theory of convective TPD instability,[1,2,10] the peaks are shifted and at the exact $\frac{3}{2}\omega_0$ value (shown in the figures by a vertical dashed line at 709.4 nm); the emission is comparable to the thermal fluctuation level. This is important because convective theory predicts no amplification and formation of $\frac{3}{2}\omega_0$ emission at the exact $\frac{3}{2}\omega_0$ value.[1,2,10] As the laser intensity approaches 10^{14} W/cm^2, the absolute TPD instability takes over, predicting finite temporal growth rates around and close to the $\omega_0/2$ value. As the characteristic five e-fold growing time mentioned in Sec. II is much less than the laser pulse duration, the TPD plasmons saturate at the same level irrespective of different growth rates around and close to the exact $\omega_0/2$ value. Consequently, the $\frac{3}{2}\omega_0$ emission gets saturated around and close to the exact $\frac{3}{2}\omega_0$ value at higher intensities which fall in the absolute TPD regime. From curves A_1 of Fig. 4 and A_2 and B_2 of Fig. 5, one notes that the signal height at exact $\frac{3}{2}\omega_0$ emission is equal to the maximum observed signal, within experimental errors. This is at variance with the convective instability theory and supports the onset of the absolute instability. As the threshold requirement of absolute TPD instability is not a sharp boundary, at a laser intensity close to this threshold, both convective and absolute instability processes may compete. To an extent this is demonstrated by the curve B_1 of Fig. 4, where one notes that at the exact $\frac{3}{2}\omega_0$ value, the signal height is far above the thermal fluctuation level but much lower than the peak value of the signal. This curve taken at $(9.8\pm2.5)\times10^{13}$ W/cm^2 satisfies fully neither the convective nor the absolute instability theory.

When we examine the profiles obtained from high-Z targets as reported in Figs. 8–13, the results become still more interesting. We note a complete absence of saturation phenomena in the same regime of laser intensity as that obtained for carbon, a low-Z target. Curves C and D of Figs. 8 and 9 are clearly in the convective instability range of laser intensities and nearly agree with the theoretical prediction. According to the absolute TPD instability theory, the signal height around and close to the exact $\frac{3}{2}\omega_0$ value should be approximately of the order of the peak value, which is not the case for curves A and B. On the other hand, they do not strictly satisfy the predictions of the convective instability theory as the signal heights, at the exact $\frac{3}{2}\omega_0$ value, are much higher than the thermal fluctuation levels. The results obtained on copper (Figs. 8–11) are well supported by those obtained on aluminum (Figs. 12 and 13). It seems that both processes might be taking place simultaneously and competing with each other, and as a result we obtain results between those predicted by the two theories.

Now let us consider the plasmon damping processes. Our theoretical results and analysis of Sec. II predict much lower spatial damping rate for copper at (1.2 ± 0.1) keV electron temperature than that for carbon at (0.5 ± 0.05) keV. As the peak-intensity saturation of the scattered radiation shows Z dependence (Figs. 4–13), Landau damping has no role to play. As discussed in Sec. II, the spatial damping rate in carbon plasma (500 eV) is about three times more than in copper (1.2 keV) or aluminum plasma (1.1 keV) at the same laser intensity of 10^{14} W/cm^2. The e-folding damping length in carbon plasma is found to be approximately 1 μm whereas it is 3 μm for copper and 3.5 μm for aluminum. Thus the faster damping of plasma waves in carbon plasma in the spatial domain before the harmonic generation region may also contribute to saturation of the scattered intensity. In copper and aluminum plasmas the wave may propagate without significant damping as compared to that for carbon and combines with the laser and, thus, the scattered intensity is not expected to be saturated.

In Figs. 14 and 15 the observed peak shifts of $\frac{3}{2}\omega_0$ emissions as a function of laser intensity are shown for carbon and copper plasmas, respectively. Theoretical peak shifts $\Delta\lambda_{ps}$ from Eq. (11), given below, by Bychenkov *et al.*[1] for s-polarized light and reported by Sinha, Kumbhare, and Gupta[10] are also plotted in the figures:

$$\Delta\lambda_{ps} = \mp(\tfrac{2}{3})\lambda_0 \left[\frac{(\frac{2}{3})y}{1 \pm (\frac{2}{3})y} \right], \tag{11a}$$

$$y = \tfrac{9}{8} \left[\frac{V_e}{c} \right]^2 (1 + 12\sin^2\theta')^{1/2}, \tag{11b}$$

where λ_0 is the incident laser wavelength and θ' is the scattering angle measured with respect to the incident beam. It is noticed that within experimental errors, the predicted and observed peak shifts reasonably, although approximately, agree. This approximation in peak shift may be taken within ± 2 Å from the average of the values represented by the three lines. Peak shifts obtained using a *p*-polarized pump beam are slightly higher than those obtained using an *s*-polarized beam and may be generally considered as nearly of the same magnitude due to both, within experimental errors. The slightly higher peak shift due to the *p*-polarized incident beam may be due to the slightly higher temperature, as absorption of *p*-polarized light in laser-produced plasma is slightly higher than that of *s*-polarized light.[41] However, it should be noted that it becomes difficult to obtain the peak shifts when the profile is saturated, as in the case of Figs. 4 and 5. In these cases we have plotted A_1', A_2', and B_2' which represent the shifts of the longer-wavelength extremities of the flat profile. We note that these points fall on the straight lines plotted in Fig. 14. It gives us a clue that in the case of flat profiles one may consider the shifts obtained from longer-wavelength extremities of the wavelength-dependent saturation domain for temperature diagnostics. It appears that in the absence of processes responsible for profile saturation, the longer-wavelength extremities of the wavelength domain represented by A_1', A_2', and B_2' might be due to pure convective TPD instability.

At this stage it is worthwhile to take appraisal of the earlier workers[8,39] (both the references pertain to the same group using a 24-beam Nd:glass laser) who considered the peak shifts of $\frac{3}{2}\omega_0$ emissions as a temperature diagnostic tool and found that the temperature estimates from the peak shifts are not very reliable. On the contrary, Sinha and Kumbhare[40] found it a reliable tool. They used both the two-foil ratio technique and the relation given by Bychenkov *et al.*[1] for the estimate of temperature from the peak shift. They reported that the agreement is reasonable considering a wide scatter in temperature estimates from various groups of workers as reported by Sakabe *et al.*[42] Here it will be worthwhile to emphasize that the earlier workers[8,39] have not given sufficient experimental details on the relevant parameters like the polarization state, the propagation vectors of the incident pump and scattered beams, and the direction of the density gradient vector, which are important for the proper analysis of the temperature estimate from the peak shifts. The detailed treatment[1] of the convective TPD instability unambiguously leads one to the conclusion that the experimental parameters mentioned above are very relevant and important, and in the absence of detailed information about them it is a bit hazardous to jump to conclusions.

ACKNOWLEDGMENTS

The authors wish to thank the heads of the Laser and Plasma Physics Divisions of the Bhabha Atomic Research Centre for official support.

[1] V. Yu. Bychenkov, A. A. Zozulja, V. P. Silin, and V. T. Tikhonshuk, Beitr. Plasma Phys. **23**, 331 (1983).
[2] V. Yu. Bychenkov, V. P. Silin, and V. T. Tikhonchuk, Fiz. Plazmy **3**, 1314 (1977) [Sov. J. Plasma Phys. **3**, 730 (1977)].
[3] R. E. Turner, D. W. Phillion, B. F. Lasinski, and E. M. Campbell, Phys. Fluids **27**, 511 (1984).
[4] E. McGoldrick and S. M. L. Sim, Opt. Commun. **39**, 172 (1981).
[5] A. A. Offenburger, A. Ng, L. Pitt, and M. R. Cervenan, Phys. Rev. A **18**, 746 (1978).
[6] H. Figueroa, C. Joshi, M. Azechi, N. A. Ebrahim, and K. G. Estabrook, Phys. Fluids **27**, 1887 (1984).
[7] R. W. Short, W. Seka, K. Tanaka, and E. A. Williams, Phys. Rev. Lett. **52**, 1496 (1984).
[8] W. Seka, B. B. Afeyan, R. Boni, L. M. Goldman, R. W. Short, and K. Tanaka, Phys. Fluids **28**, 2570 (1985).
[9] V. Aboites, T. P. Hughes, E. McGoldrick, S. M. L. Sim, S. J. Karttunen, and R. G. Evans, Phys. Fluids **28**, 2555 (1985).
[10] B. K. Sinha, S. R. Kumbhare, and G. P. Gupta, Phys. Rev. A **36**, 4859 (1987).
[11] S. J. Karttunen, Laser Part. Beams **3**, 157 (1985).
[12] H. C. Pant, K. Eidmann, P. Sachsenmaier, and R. Sigel, Opt. Commun. **16**, 396 (1976).
[13] A. I. Avrov, V. Yu. Bychenkov, O. N. Krokhin, V. V. Dustavalov, A. A. Rupasov, V. P. Silin, G. V. Sklizkov, V. T. Tikhonchuk, and A. S. Shikanov, Zh. Eksp. Teor. Fiz. **72**, 970 (1977) [Sov. Phys.—JETP **45**, 507 (1977)].
[14] V. V. Alexandrov, Zh. Eksp. Teor. Fiz. **71**, 1826 (1976) [Sov. Phys.—JETP **44**, 958 (1976)].
[15] M. N. Rosenbluth, Phys. Rev. Lett. **29**, 565 (1972).
[16] I. F. Drake and Y. C. Lee, Phys. Rev. Lett. **31**, 1197 (1973).
[17] R. White, P. K. Kaw, P. Presme, M. N. Rosenbluth, G. Laval, R. Huff, and R. Varma, Nucl. Fusion **14**, 45 (1974).
[18] C. S. Liu, in *Advances in Plasma Physics*, edited by A. Simon and W. B. Thomson (Wiley, New York, 1976), Vol. 6, pp. 174 and 177; C. S. Liu and M. N. Rosenbluth, Phys. Fluids **19**, 967 (1976).
[19] R. N. Franklin, Rep. Prog. Phys. **40**, 1369 (1977).
[20] R. N. Franklin, S. M. Hamberger, G. Lampis, and G. J. Smith, Phys. Rev. Lett. **27**, 1119 (1971).
[21] S. J. Karttunen, Phys. Rev. A **23**, 2006 (1981).
[22] K. Tanaka, W. Seka, L. M. Goldman, M. C. Richardson, R. W. Short, J. M. Soures, and E. A. Williams, Phys. Fluids **27**, 2187 (1984).
[23] J. Meyer and H. Houtman, Phys. Rev. Lett. **53**, 1344 (1984).
[24] M. A. Greenspan, C. Ekdahl, J. D. Sethian, and C. B. Wharton, Phys. Fluids **23**, 205 (1980).
[25] F. W. Perkins and J. Flick, Phys. Fluids **14**, 2012 (1971).

[26]B. F. Lasinski and A. B. Langdon, Lawrence Livermore National Laboratory Report No. UCRL-50021-77 (1977), pp. 4–49 (unpublished).
[27]A. Simon, R. W. Short, E. A. Williams, and T. Dewandre, Phys. Fluids **26**, 3107 (1983).
[28]T. J. M. Boyd, Can. J. Phys. **64**, 944 (1986).
[29]J. A. Bittencourt, *Fundamentals of Plasma Physics* (Pergamon, Oxford, 1986), pp. 427 and 522.
[30]W. M. Stacey, *Fusion–An Introduction to the Physics and Technology of Magnetic Confinement Fusion* (Wiley, New York, 1984), p. 30.
[31]J. W. Shearer and W. S. Barnes, in *Laser Interaction and Related Plasma Phenomena,* edited by H. J. Schwartz and H. Hora (Plenum, New York, 1971), Vol. 1, p. 314.
[32]D. Mosher, Phys. Rev. A **10**, 2330 (1974).
[33]P. Mora, Phys. Fluids **25**, 1051 (1982).
[34]B. K. Sinha and N. Gopi, Phys. Fluids **23**, 1704 (1980).
[35]B. K. Sinha, J. Phys. D **13**, 1253 (1980).
[36]S. D. Tabatabaei and B. J. MacGowan, Rutherford Appleton Laboratory Annual Report No. RAL-85-047 (1985), p. A1.21 (unpublished).
[37]J. L. Bobin, Phys. Rep. **122**, 236 (1985).
[38]J. H. Gardner, M. J. Herbst, F. C. Young, J. A. Stamper, S. P. Obenschain, C. K. Manka, K. J. Kearney, J. Grun, D. Dutson, and P. G. Burkhalter, Phys. Fluids **29**, 1305 (1986).
[39]L. M. Goldman, W. Seka, K. Tanaka, R. Short, and A. Simon, Can. J. Phys. **64**, 969 (1986).
[40]B. K. Sinha and S. R. Kumbhare, Plasma Phys. Contr. Nucl. Fusion **29**, 1037 (1987).
[41]T. P. Hughes, in *Laser-Plasma Interactions,* Proceedings of the Twentieth Scottish Universities Summer School in Physics, edited by R. A. Cairns and J. J. Sanderson (Saint Andrews, Scotland, 1979), p. 70.
[42]S. Sakabe, T. Mochizuki, T. Yabe, K. Mima, and C. Yamanaka, Phys. Rev. A **26**, 2159 (1982).